 CMES, vol.34, no.1, pp.33-53, 2008

Wave Modes of An Elastic Tube Conveying Blood

Shueei-Muh Lin[1,3], Sen-Yung Lee[2], Cheng-Chuan Tsai[2], Chien-Wi Chen[2]
Wen-Rong Wang[3] and Jenn-Fa Lee[3]

Abstract: The conventional theories for circulation of arteries are emphasized on fluid behavior or some simplified models for experimental utility. In this study, a new mathematical theory is proposed to describe the wave propagation through the elastic tube filled with viscous and incompressible fluid. The radial, longitudinal and flexural vibrations of a tube wall are introduced simultaneously. Meanwhile, the linearlized momentum and continuity equations of tube flow field are expressed in the integral form. Based on these considerations, three wave modes are obtained simultaneously. These wave modes are the flexural, Young and Lamb modes, respectively. The characteristics of these modes are clearly demonstrated. In the literature, according to different assumptions, the Young and Lamb modes were independently derived. It is usually thought that all the energies of the Young mode and the Lamb mode were transmitted through the liquid and the tube, respectively. Because these conventional models are over simplified, the corresponding investigations are incomplete and inaccurate. In this study, it is found that almost all the energies of the flexural and Lamb modes are transmitted through the tube. However, only about sixty percent of the energy of the Young mode is transmitted through the liquid. Finally, the effects of several important parameters on the dispersion curves and the energy transmissions of these modes are investigated.

Key words: artery, dispersion curve, energy propagation, and wave mode.

1 Introduction

No matter animals or human beings, the blood circulation plays an important role in maintaining body working well. Many scientists investigated the heart vascular system, and proposed several theories and models to explain the performances of

[1] Corresponding author.
[2] Department of Mechanical Engineering, National Cheng Kung University, Tainan, Taiwan 701, Republic of China
[3] Department of Mechanical Engineering Department, Kun Shan University, Tainan, Taiwan 710-03, Republic of China

the blood circulation system.

Since Harvey (1628) introduced the concept of the blood circulation, scientists have developed several vital theories. Hales (1733) introduced the Winkessel model. The Winkessel model regards the whole arteries system as an elastic cavity. If the heart contracts, the cavity expands. In contrast, if the heart expends, the cavity recovers to original volume. But the Winkessel model is only suitable for predicting quantity of each contraction, and fails to evaluate flow velocity. Assuming a steady and laminar flow and a rigid tube, the Poiseuille's equation explains the physical characteristics of the blood capillary (1989). Fishman and Richards (1964) applied the Poiseuille's equation in their experiment. However, the Poiseuille's equation neglects that the pressure wave propagation in fluid creates an oscillation motion of the wall in a radial direction. Moens and Korteweg (1878) developed a simple equation called as the Moens-Korteweg equation to predict the pressure wave velocity in long straight thin tube filled with an inviscid fluid. Because the effects of viscosity of fluid, inertial and shear and bending deformations of a tube are neglected, the Moens-Korteweg equation can derive the wave velocity only. Bergal (1961) modified the Moens-Korteweg equation for a thick-walled tube. Womersley (1955) considered a thin walled tube and the linearized Navier-Stokes equations that the nonlinear convective acceleration terms were neglected. Meanwhile, the radial vibration of tube wall was neglected. According to these assumptions, only the Young and Lamb modes were found. Moreover, the Young and Lamb modes represent the pressure wave modes propagating in the fluid and in the wall, respectively. Note that neglecting the radial vibration of tube does not match the real wave performance of artery. Tsangaris and Drikakis (1989) used the shell theory and the Navier-Stokes equation to simulate the pressure wave traveling in anisotropic elastic tube. The model neglected the effects of the radial vibration and the moving boundary between the tube and the fluid. Demiray (1997) considered the dynamic relation between the inner pressure and the radial oscillation of a tube. But the effect of flexural deformation of a tube and the viscosity of fluid were neglected. Then only the Young mode which represent pressure wave propagating in the fluid could be derived. Wang *et al*. (1997, 2000) considered an artery system as a transmission system of the blood pressure wave. When the wave frequency of the artery was consistent to the natural frequency of a tissue, the transmission efficiency was the best. This model is called as the resonant model. However, this model was derived too roughly to investigate the effects of the pre-pressure, the flow velocity and the flexural and axial vibrations. Sarkar and Sonti (2007) studied the wavenumber of a fluid-filled cylindrical shell vibrating in the axisymmetric mode. But the coupled flow motion of fluid was not considered. Because the fluid-structure interaction (FSI) play an important role in cardiovascular disease initiation and development, Yang *et al.* (2007) investigated the non-wave FSI of arteries by using the commercial ADINA software. The maximum shear stress and the pressure distribution in the arteries were presented.

In this paper, a new mathematical model is proposed to describe the wave propagation through the isotropic elastic tube filled with viscous and incompressible fluid. The radial, longitudinal and flexural vibrations of a tube wall will be investigated simultaneously. The effects of several parameters on the dispersion curves and the energy transmissions of the three modes are investigated. Moreover, the characteristics of the three modes will be clearly discussed.

2 Governing equation of motion

2.1 Motion of an elastic tube

Consider an artery as uniform isotropic elastic tube. The tube is filled with the blood. The blood flow field in the tube is assumed as steady and laminar. Using the Donnell's shell theory simulates the motion of the blood tube. Donnell's assumptions (1974) are as follows:

a. The in-plane deflection due to bending is neglected.

b. The rotatory inertia is neglected.

c. The shear effect in the r-plane is neglected.

d. The effect of tube bending is considered.

e. The plane cross section of a tube wall remains plane during deformation.

It is different to a conventional thin-walled tube simulated by using the membrane theory (1968). In the Donnell's model, the strain-displacement relation for a tube can be expressed as

$$\varepsilon_\theta = \frac{1}{R}\frac{\partial u_\theta}{\partial \theta} + \frac{u_r}{R} \tag{1}$$

$$\varepsilon_z = \frac{\partial u_z}{\partial z} \tag{2}$$

$$\gamma_{\theta z} = \frac{\partial u_\theta}{\partial z} + \frac{1}{R}\frac{\partial u_z}{\partial \theta} \tag{3}$$

$$\kappa_z = -\frac{\partial^2 u_r}{\partial z^2} \tag{4}$$

$$\kappa_\theta = -\frac{1}{R^2}\frac{\partial^2 u_r}{\partial \theta^2} \tag{5}$$

$$\kappa_{z\theta} = -2\frac{1}{R}\frac{\partial^2 u_r}{\partial \theta \partial z} \tag{6}$$

where u_r, u_θ, and u_z are displacements in r-direction, in θ-direction and in z-direction respectively. ε_r, ε_θ and ε_z are normal strain in r-direction, in θ-direction and in z-direction respectively. $\gamma_{\theta z}$ is shearing strain on $\theta - z$ plane, κ_z is bending curvature perpendicular to z-plane along θ-direction, κ_θ is bending curvature perpendicular to θ-plane along z-direction, $\kappa_{z\theta}$ is torsional curvature perpendicular to θ-plane along z-direction or perpendicular to z-direction along θ-plane, R is the radius of elastic cylinder.

Moreover, the relations among the forces, the moments, the strain and the curvatures are (1974)

$$N_z = \frac{Eh}{1-\nu^2}\left(\varepsilon_z + \nu\varepsilon_\theta\right) \tag{7}$$

$$N_\theta = \frac{Eh}{1-\nu^2}\left(\varepsilon_\theta + \nu\varepsilon_z\right) \tag{8}$$

$$N_{\theta z} = Gh\gamma_{\theta z} \tag{9}$$

$$M_z = \frac{Eh^3}{12\left(1-\nu^2\right)}\left(\kappa_z + \nu\kappa_\theta\right) \tag{10}$$

$$M_\theta = \frac{Eh^3}{12\left(1-\nu^2\right)}\left(\kappa_\theta + \nu\kappa_z\right) \tag{11}$$

$$M_{\theta z} = \left(\frac{1-\nu}{2}\right)\frac{Eh^3}{12\left(1-\nu^2\right)}\kappa_{\theta z} \tag{12}$$

where N_θ and N_z are normal force on θ-plane and z-plane per unit length respectively. $N_{\theta z}$ is shearing force perpendicular to θ-plane along z-direction or perpendicular to z-plane along θ-direction per unit length, M_θ and M_z are bending moment perpendicular to θ-plane along z-direction and one perpendicular to z-plane along θ-direction per unit length respectively. E is the Young's modulus, G is the shear modulus, ν is the Poisson's ratio, h is the thickness of the cylinder wall. The equilibrium equations of motion are (1974)

$$\frac{\partial N_z}{\partial z} + \frac{1}{R}\frac{\partial N_{\theta z}}{\partial \theta} + q_z = \rho_s h\frac{\partial^2 u_z}{\partial t^2} \tag{13}$$

$$\frac{\partial N_{z\theta}}{\partial z} + \frac{1}{R}\frac{\partial N_\theta}{\partial \theta} = 0 \tag{14}$$

$$\frac{\partial^2 M_z}{\partial z^2} + 2\frac{1}{R}\frac{\partial^2 M_{\theta z}}{\partial\theta\partial z} + \frac{1}{R^2}\frac{\partial^2 M_\theta}{\partial\theta^2} - \frac{N_\theta}{R} + q_r = \rho_s h\frac{\partial^2 u_r}{\partial t^2} \tag{15}$$

where t is the time variable, ρ_s is the density of the tube wall, q_z is the external force in z-direction, q_r is the external force in r-direction. Considering the axial symmetry, the displacement $u_\theta = 0$ and the parameters are independent of the θ-axis. Thus the equation of motion (14) is negligible. Substituting Eqs. (1-12) into Eqs. (13) and (15), one can derive the equation of motion of an elastic tube (1968)

$$\frac{\partial^2 u_z}{\partial z^2} + \frac{\nu}{R}\frac{\partial u_r}{\partial z} = \frac{1-\nu^2}{E}\rho_s\frac{\partial^2 u_z}{\partial t^2} - \frac{1-\nu^2}{Eh}\tau_r(z,t) \tag{16}$$

$$\frac{\nu}{R}\frac{\partial u_z}{\partial z} + \frac{h^2}{12}\frac{\partial^4 u_r}{\partial z^4} + \frac{u_r}{R^2} = -\frac{1-\nu^2}{E}\rho_s\frac{\partial^2 u_r}{\partial t^2} + \frac{1-\nu^2}{Eh}p(z,t) \tag{17}$$

where τ_r and p are the shear stress and the liquid pressure at the wall, respectively. They are derived in the next section.

2.2 Coupled motion of fluid and tube

In general, the blood flow velocity in a tube is small. The corresponding Reynold's number is low. Thus the flow filed is laminar. Moreover, when a wave propagates through a tube, the flow field in the tube is assumed to be well developed. The velocity distribution is expressed as

$$\eta = \eta_{\max}(z,t)\left[1-\left(\frac{r}{R}\right)^2\right], \tag{18}$$

where $\eta_{\max}$ is the maximum flow velocity at the center of tube. The average shear stress at the wall along a tube length of dz is

$$\tau_r = \mu\frac{\partial}{\partial r}\left(\eta + \frac{1}{2}\frac{\partial\eta}{\partial z}dz\right)_{wall} \tag{19}$$

Substituting Eq. (18) into Eq. (19) and Eq. (16), one obtains

$$\frac{\partial^2 u_z}{\partial z^2} + \frac{\nu}{R}\frac{\partial u_r}{\partial z} = \frac{1-\nu^2}{E}\rho_s\frac{\partial^2 u_z}{\partial t^2} - \frac{2\mu\left(1-\nu^2\right)}{REh}\eta_{\max} \tag{20}$$

It is well known that the conservation of linear momentum for liquid is

$$F_b + F_s = \frac{\partial}{\partial t}\int_{c.v.}\vec{v}\rho_f dV + \int_{c.s.}\vec{v}\rho_f\vec{v}\cdot\hat{n}dA \tag{21}$$

where the body force F_b is negligible here. As shown in Figure 1, the surface force is

$$F_s = -\left(p+\frac{\partial p}{\partial z}dz\right)\cdot\pi\left(R+u_r+\frac{\partial u_r}{\partial z}dz\right)^2 + p\pi\left(R+u_r\right)^2 - \tau_w\cdot 2\pi r\cdot dz \tag{22}$$

Where $\vec{v}$ is the flow velocity, ρ_f is the density of fluid, V is the volume of the fluid element, A is the surface area. $\hat{n}$ Is the normal direction of surface. Substituting the pressure and the shear stress at the wall into Eq. (21) and considering a small amplitude, i.e., $u_r \ll R$, the momentum equation can be written as

$$\left(-R^2-2Ru_r\right)\frac{\partial p}{\partial z} - 2Rp\frac{\partial u_r}{\partial z} - 4\mu\eta_{\max} = \frac{1}{2}R\rho_f\frac{\partial}{\partial t}\left[\eta_{\max}R^2 + 2R\eta_{\max}u_r\right] + \frac{1}{3}\rho_f\left(2R\eta_{\max}^2\frac{\partial u_r}{\partial z} + \left(2\eta_{\max}R^2 + 4\eta_{\max}Ru_r\right)\frac{\partial \eta_{\max}}{\partial z}\right) \tag{23}$$

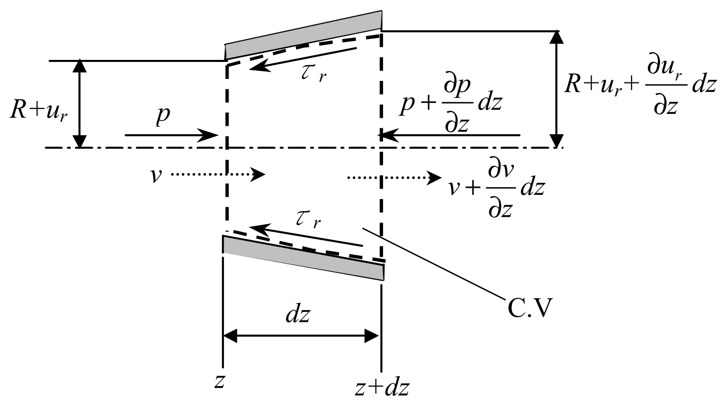

Figure 1: Control volume of blood flow in a circular cylinder.

Meanwhile, if the amplitude of wave is small, the mass conservative equation can be expressed as

$$\pi\rho\left(2R\eta_{\max}\frac{\partial u_r}{\partial z} + \left(R^2+2Ru_r\right)\frac{\partial \eta_{\max}}{\partial z}\right) + 4\pi R\rho_f\frac{\partial u_r}{\partial t} = 0. \tag{24}$$

In this study, a new mathematical model simulating the wave propagation through an elastic thin-walled tube conveying a liquid has been constructed completely. The new wave propagation model is composed of the coupled characteristic equations (17, 20, 23, 24).

3 Solution method

Consider that there exists a pre-stressed pressure and a flow rate in the tube. The pressure and the velocity are composed of the factors of the steady state and the wave perturbation as follows:

$$p(z,t) = p_{0,z}(z) + p_1(z,t), \quad \eta_{\max}(z,t) = \eta_{\max_0}(z) + \eta_{\max_1}(z,t), \tag{25}$$

where $p_{0,z}$ is the pre-stressed steady pressure at the position of z, p_1 the disturbed wave pressure, $\eta_{\max_0}$ the average maximum flow velocity corresponding the given flow rate, and $\eta_{\max_1}$ the disturbed wave flow velocity.

In general, a steady pressure loss Δp through a tube is determined by using the Darcy-Weisbach Equation as follows:

$$\Delta p = f\frac{L}{D}\frac{\rho_f \eta_a^2}{2} \tag{26}$$

where η_a is the average flow velocity which is determined via Eq. (18) and $\eta_a = \eta_{\max_0}/2$. L is the tube length, D is the diameter of the tube, and f is the friction factor. In this study, because the flow is laminar, the friction factor $f = 64/Re$. Substituting it back into Eq. (26), the relation between the velocity and the difference between the pressures at the position of 0 and z is

$$p_{0,0} - p_{0,z} = \frac{64\mu\eta_{\max_0}z}{R^2}. \tag{27}$$

In general, because the elastic wave propagation is small, the disturbed wave pressure and velocity $\{p_1, \eta_{\max_1}\}$ are small. Substituting Eqs. (25) and (27) into the coupled characteristic equations (17, 20, 23, 24) and considering the condition of small wave propagation, the linearlized coupled characteristic equations are obtained

$$\frac{\partial^2 u_z}{\partial z^2} + \frac{\nu}{R}\frac{\partial u_r}{\partial z} = \frac{1-\nu^2}{E}\rho_s\frac{\partial^2 u_z}{\partial t^2} - \frac{2\mu\left(1-\nu^2\right)}{REh}\left(\eta_{\max_0} + \eta_{\max_1}\right) \tag{28}$$

$$\frac{\nu}{R}\frac{\partial u_z}{\partial z} + \frac{h^2}{12}\frac{\partial^4 u_r}{\partial z^4} + \frac{u_r}{R^2} = -\frac{1-\nu^2}{E}\rho_s\frac{\partial^2 u_r}{\partial t^2} + \frac{1-\nu^2}{Eh}\left(p_{0,0} + p_1\right) \tag{29}$$

$$\begin{aligned} &-\frac{64\mu\eta_{\max_0}}{R^2} - \frac{\partial p_1}{\partial z} - \frac{128\mu\eta_{\max_0}}{R^3}u_r - \frac{2p_{0,0}}{R}\frac{\partial u_r}{\partial z} - \frac{4}{R^2}\mu\eta_{\max_0} - \frac{4}{R^2}\mu\eta_{\max_1} \\ &= \frac{1}{2}\rho_f\frac{\partial \eta_{\max_1}}{\partial t} + \frac{1}{R}\rho_f\eta_{\max_0}\frac{\partial u_r}{\partial t} + \frac{2}{3R}\rho_f\eta_{\max_0}^2\frac{\partial u_r}{\partial z} + \frac{2}{3}\rho_f\eta_{\max_0}\frac{\partial \eta_{\max_1}}{\partial z} \end{aligned} \tag{30}$$

$$\frac{2}{R}\eta_{\max_0}\frac{\partial u_r}{\partial z}+\frac{\partial \eta_{\max_1}}{\partial z}+\frac{4}{R}\frac{\partial u_r}{\partial t}=0 \tag{31}$$

The wave solutions of the linearlized coupled characteristic equations (28-31) can be expressed as

$$\eta_{\max_1}=\bar{\eta}e^{i(kz-\omega t)},\quad p_1=\bar{p}e^{i(kz-\omega t)},$$

$$u_r=U_{r0}(z)+U_r e^{i(kz-\omega t)},\quad u_z=U_{z0}(z)+U_z e^{i(kz-\omega t)} \tag{32}$$

where $\bar{\eta}$ is the amplitude of the disturbed flow velocity due to wave propagation, $\bar{p}$ the amplitude of the disturbed pressure, U_{r0} the static deflection in r-direction due to pre-stressed, U_{z0} the static deflection in z-direction, U_r the amplitude of the vibration in r-direction due to wave propagation, U_z the amplitude of the vibration in z-direction, $k$the wave number, and ω the angular frequency.

Substituting the solution (32) into the linear characteristic equations (28-31), the general system is divided into dynamic and static subsystems as following:

(a) Dynamic subsystem is composed of four following equations:

$$\bar{p}=\left[-\rho_s\omega^2+\frac{Eh}{(1-\nu^2)}\left(\frac{1}{R^2}+\frac{h^2}{12}k^4\right)\right]U_r+i\frac{k\nu Eh}{R(1-\nu^2)}U_z \tag{33}$$

$$\bar{\eta}=\frac{2}{R}\left(\frac{2\omega}{k}-\eta_{\max_0}\right)U_r \tag{34}$$

$$(ik)^2U_z+ik\frac{\nu}{R}U_r=(-i\omega)^2\frac{1-\nu^2}{E}\rho_sU_z-\frac{2\mu\left(1-\nu^2\right)}{REh}\bar{\eta} \tag{35}$$

$$-ik\bar{p}-\frac{128\mu\eta_{\max_0}}{R^3}U_r-i\frac{2kp_{0,0}}{R}U_r-\frac{4}{R^2}\mu\bar{\eta}=-i\omega\frac{1}{2}\rho_f\bar{\eta}-i\omega\frac{1}{R}\rho_f\eta_{\max_0}U_r$$
$$+ik\frac{2}{3R}\rho_f\eta_{\max_0}^2U_r+ik\frac{2}{3}\rho_f\eta_{\max_0}\bar{\eta} \tag{36}$$

(b) Static subsystem is composed of three following equations:

$$U_{z0}''+\frac{\nu}{R}U_{z0}'=0 \tag{37}$$

$$\frac{\nu}{R}U_{z0}'+\frac{h^2}{12}U_{r0}^{(4)}+\frac{1}{R^2}U_{r0}=\frac{1-\nu^2}{Eh}p_{0,0} \tag{38}$$

$$-\frac{64\mu\eta_{\max_0}}{R^2}-\frac{128\mu\eta_{\max_0}}{R^3}U_{r0}-\frac{2}{R}p_{0,0}U_{r0}'=0 \tag{39}$$

Note that Eqs. (37-39) are the relations among the static displacements $\{U_{r,0},\ U_{z,0}\}$, the pre-pressure $p_{0,0}$ and flow velocity $\eta_{\max_0}$. On the other hand, Eqs. (33-36) are the characteristic equations due to wave propagation. Substituting Eqs. (33-34) into Eqs. (35-36), one can obtain the following equation in terms of the variables U_z and U_r

$$\begin{bmatrix}\alpha_{11} & \alpha_{12}\\ \alpha_{21} & \alpha_{22}\end{bmatrix}\begin{bmatrix}U_z\\ U_r\end{bmatrix}=\begin{bmatrix}0\\ 0\end{bmatrix} \tag{40}$$

where

$$\begin{aligned}
\alpha_{11} =& \omega^2 k\frac{1-\nu^2}{E}\rho_s - k^3\\
\alpha_{12} =& ik^2\frac{\nu}{R}+\omega\frac{8\mu\left(1-\nu^2\right)}{R^2Eh}-k\frac{4\mu\eta_{\max_0}\left(1-\nu^2\right)}{R^2Eh}\\
\alpha_{21} =& -\frac{\nu}{R}k^3\\
\alpha_{22} =& -\left(-\frac{16\mu}{R^2}+i2\omega\rho_f\right)\frac{\omega\left(1-\nu^2\right)}{REh}+\frac{\left(1-\nu^2\right)}{Eh}\left[i\frac{8\omega\rho_f\eta_{\max_0}}{3R}+\frac{120\mu\eta_{\max_0}}{R^3}\right]k\\
&+i\frac{\left(1-\nu^2\right)}{Eh}\left[-\rho_s\omega^2+\frac{Eh}{R^2\left(1-\nu^2\right)}-\frac{2\rho_f\eta^2_{\max_0}}{3R}+\frac{2p_{0,0}}{R}\right]k^2+i\frac{h^2}{12}k^6
\end{aligned} \tag{41}$$

If U_z and U_r are zero, it is trivial. Thus the determinant $\left|\alpha_{ij}\right|$ must be zero. It is the characteristic equation and expressed as follows:

$$k^8a_{r8}+k^6a_{r6}+k^4a_{r4}+k^3\left(a_{r3}+ia_{i3}\right)+k^2\left(a_{r2}+ia_{i2}\right)\ +k\left(a_{r1}+ia_{i1}\right)+\left(a_{r0}+ia_{i0}\right)=0 \tag{42}$$

where

$$\begin{aligned}
a_{r8} &= -\frac{h^2}{12}\\
a_{r6} &= \frac{\omega^2\rho_s h^2\left(1-\nu^2\right)}{12E}\\
a_{r4} &= \frac{\left(1-\nu^2\right)}{Eh}\left[\rho_s\omega^2+\frac{2\rho_f\eta^2_{\max_0}}{3R}-\frac{2p_{0,0}}{R}\right]-\frac{1-\nu^2}{R^2}\\
a_{r3} &= \frac{-8\omega\rho_f\eta_{\max_0}\left(1-\nu^2\right)}{3REh}\\
a_{i3} &= \frac{4\mu\eta_{\max_0}\left(1-\nu^2\right)\left(30+\nu\right)}{R^3Eh}
\end{aligned}$$

$$
\begin{aligned}
a_{r2} =& \frac{2\omega^2\rho_f\left(1-\nu^2\right)}{REh} \\
&+ \frac{\omega^2\rho_s\left(1-\nu^2\right)^2}{E^2h}\left[\left(-\rho_s\omega^2+\frac{Eh}{R^2\left(1-\nu^2\right)}\right)-\frac{2\rho_f\eta_{\max_0}^2}{3R}+\frac{2p_{0,0}}{R}\right] \\
a_{i2} =& \frac{8\omega\mu\left(1-\nu^2\right)}{R^3Eh}\left(2-\nu\right) \\
a_{r1} =& \frac{8\omega^3\rho_f\eta_{\max_0}\rho_s\left(1-\nu^2\right)^2}{3RE^2h} \\
a_{i1} =& -\frac{120\omega^2\mu\eta_{\max_0}\rho_s\left(1-\nu^2\right)^2}{R^3E^2h} \\
a_{r0} =& \frac{-2\omega^4\rho_s\rho_f\left(1-\nu^2\right)^2}{RE^2h} \\
a_{i0} =& \frac{-16\omega^3\rho_s\mu\left(1-\nu^2\right)^2}{R^3E^2h}
\end{aligned} \tag{43}
$$

The wave number k of a wave mode can be determined via Eq. (42). Substituting it back into Eq. (40), one can derive the mode shape $\{U_r, U_z\}$ of the tube. Further, substituting the mode shape into Eqs. (1-3) and (33-34), the corresponding strains, the pressure and the flow velocity of the wave mode are derived. Finally, the corresponding stresses of the tube can be determined by using the Hook's law.

4 Energy propagation

It is well known that the wave energy is stored in both the tube and the liquid. Milnor (1989) found by experiment that for an *in situ* artery, over 90% of the energy is stored in the arterial wall and less than 10% is stored in the blood flow. However, the mechanism about the wave energy propagation has not been completely and clearly investigated yet. In this study, the energy transmission via different mode is investigated.

The energy propagation stored in the liquid is a product of the pressure p and the flow velocity η and expressed as following:

$$E_l = \int_A \langle p(t), \eta(t)\rangle\, dA, \tag{44}$$

where the average energy rate is $\langle p(t), \eta(t)\rangle = \int_0^T Re(p)Re(\eta)\,dt/T$. The energy in the tube is composed of the normal strain energy and the shear strain energy and is written as

$$E_t = \int_A \left\langle \sigma_x, \frac{\partial u_x}{\partial t}\right\rangle dA + \int_A \left\langle \tau_{rx}, \frac{\partial u_r}{\partial t}\right\rangle dA, \tag{45}$$

where the average normal strain energy is $\langle \sigma_x, \partial u_x/\partial t\rangle = \int_0^T Re(\sigma_x) Re[\partial u_x/\partial t]\, dt/T$ and the average shear strain energy is $\langle \tau_{rx}, \partial u_r/\partial t\rangle = \int_0^T Re(\tau_{rx}) Re[\partial u_r/\partial t]\, dt/T$. Substituting the pressure and the flow velocity of a wave mode into Eq. (44) and the stresses and the displacements of a wave mode into Eq. (45), the corresponding energy propagations stored in the blood liquid and the tube can be obtained.

5 Numerical results

Given a wave frequency ω, one can easily find four sets of conjugated complex wave numbers of Eq. (42), $k_n(\omega) = k_{r,n}(\omega) \pm i k_{i,n}(\omega)$, $n = 1,2,3,4$. Each set of conjugated roots represent both a forward wave and a backward wave, respectively. If $k_{i,n}$ is positive, the wave amplitude decays with a forward wave. But if $k_{i,n}$ is negative, the wave amplitude increases with a forward wave. This solution is trivial. Based on these facts, one can obtain the dispersion curves of several wave modes. In this study, the wave propagation through both the blood and the artery are considered [Cox. 1990]. One finds that three sets of conjugated roots are reasonable, but one is trivial. Each reasonable solution represents one wave mode. In other words, three kinds of wave modes shown in Figure 2 can be found simultaneously by using this proposed theory.

Figure 2a shows the displacements of the points {p, Q} at the inner and outer walls of tube for the first mode. It is found from the numerical result that the longitudinal displacement U_z at the middle of tube thickness is very small. In addition, the phenomenon can be also observed from Figure 2a by averaging the longitudinal displacements U_z of the points {p, Q}. It is concluded that the first mode is dominated by a flexural motion of a tube wall. In order to investigate the detail of energy propagation through blood and tube, the ratio of the amplitude of fluid velocity to that of the dominated radial displacement of tube, $\bar{\eta}/U_r$, is determined and found to be small to about 1.8 (1/sec) for the first mode. Because the bending deflection of tube is large and the fluid velocity is small, the majority of the wave energy must be propagated through the tube in the bending motion. Figure 2b shows the second and third mode shapes. The second mode is usually called as the Young mode. The second mode is a longitudinal motion of a tube accompanying small radial motion of a tube and relatively very large amplitude of fluid velocity. The ratio of the amplitude of fluid velocity to that of the dominated longitudinal displacement of tube, $\bar{\eta}/U_z$, is about 50 (1/sec). Therefore, the majority of the wave energy must be propagated through fluid in the pressure wave motion. The third mode is usually called as the Lamb mode. The third mode is a large longitudinal motion of a tube accompanying a negligible radial motion of a tube and small amplitude of fluid velocity. The ratio of the amplitude of fluid velocity to that of the longitudinal displacement of tube, $\bar{\eta}/U_z$, is about 0.1 (1/sec). Therefore, the majority of the wave energy must

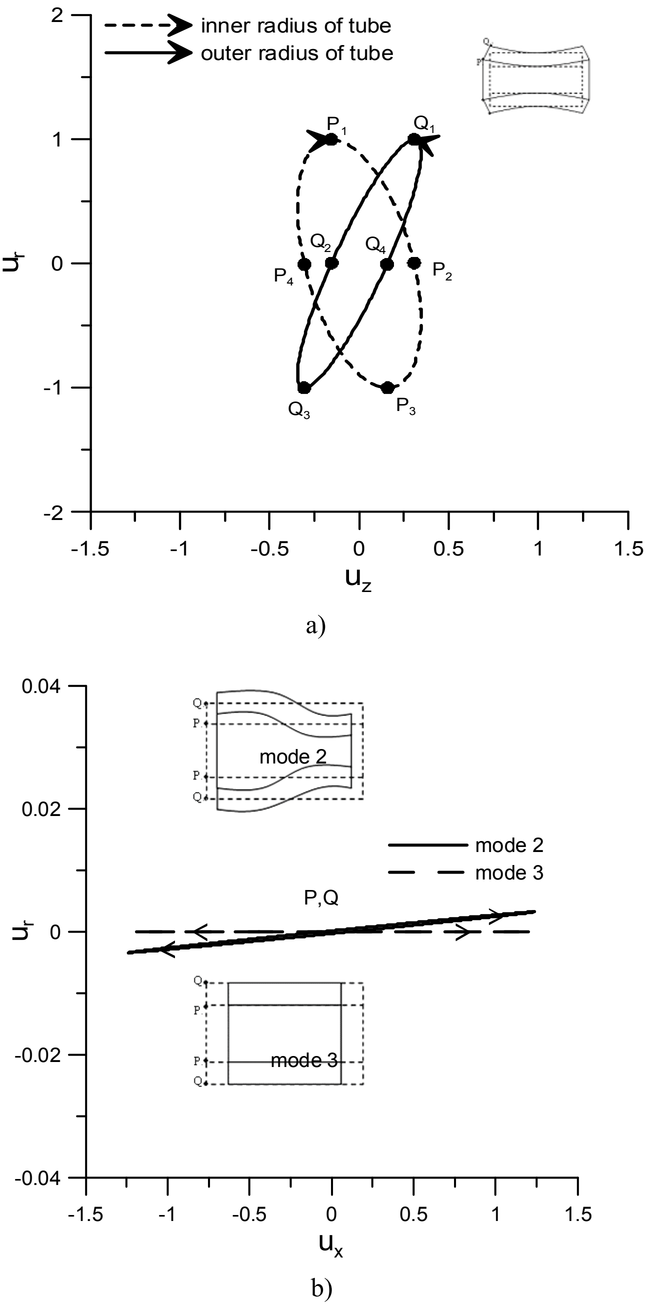

Figure 2: Three kinds of mode shapes. [Poisson Ratioν=0.5, Young's Modulus E=3 MPa, outer radius of tube R_o=0.23 cm, thickness of tube wall h = 0.03 cm, density of tube ρ_t = 1100 Kg/m^3, density of fluid ρ_f= 1056 Kg/m^3, viscosity $\mu = 3.5\times10^{-3}$ N·Es/m^2, pre-pressure p_0=10 kPa]. a): mode 1; b): modes 2 and 3.

be propagated through the tube in the longitudinal motion.

Based on the relations (44) and (45), one can determine the quantities of energy transmission through the tube and the liquid. As shown in Figure 3, all the energies of the first and third modes are transmitted almost through the tube. However, only about forty percent of the energy of the second mode is transmitted through the tube. The detailed are expressed as follows:

It has been found that the first mode is a wall flexural motion accompanying with small fluid velocity. Because both the bending rigidity and the flexural deformation of a tube wall are large, almost all the wave energy is transmitted through the tube. Similarly, the third mode is with a large longitudinal motion of a tube accompanying with a negligible radial motion and small flow velocity. Therefore, almost all the wave energy is also transmitted through the tube. However, the second mode is a large longitudinal motion of a tube accompanying with small radial motion and very large flow velocity. It is well known that the flexural and longitudinal motions of tube are neglected in the conventional Moens-Korteweg model for determining the Young mode. According to this simplification, it is usually concluded that the Young mode represents pressure wave propagation in the fluid and all the energy is transmitted through the liquid. It is not reasonable. In this study, Figure 3 shows that about forty per cent of the wave energy is transmitted through the tube.

Figure 4 shows the relations between the wave speed and the wave frequency for the three modes. It is observed that the wave speed of the first mode is less than those of the second and third modes. Increasing the wave frequency from zero greatly increases the wave speed of the three modes. When the wave frequency is larger than 10 (rad/s), the wave speeds of the second and third modes are almost constant, but that of the first mode always increases with the wave frequency. Conventionally, the general system is usually simplified into a limiting case to determine independently the second mode or the third. By using these conventional and over-simplified theories, the corresponding wave speeds are independent to the wave frequency.

It is well known that the wave speed of the Young mode in the Moens-Korteweg model is $c_0 = \sqrt{Eh/\left[2\left(R-h/2\right)\rho_f\right]}$. Obviously, the corresponding wave speed is independent to the wave frequency. This model is not applicable for determining the energy propagation. Moreover, increasing the ratio h/R greatly increases the wave speed. Considering the ratio h/R from 0.04 to 0.14, it is observed that the numerical results in the Moens-Korteweg model are slightly larger than those determined by using the present method especially for the larger ratio h/R. It is because the effects of kinetic viscosity and flexural deformation are neglected in the Moens-Korteweg model.

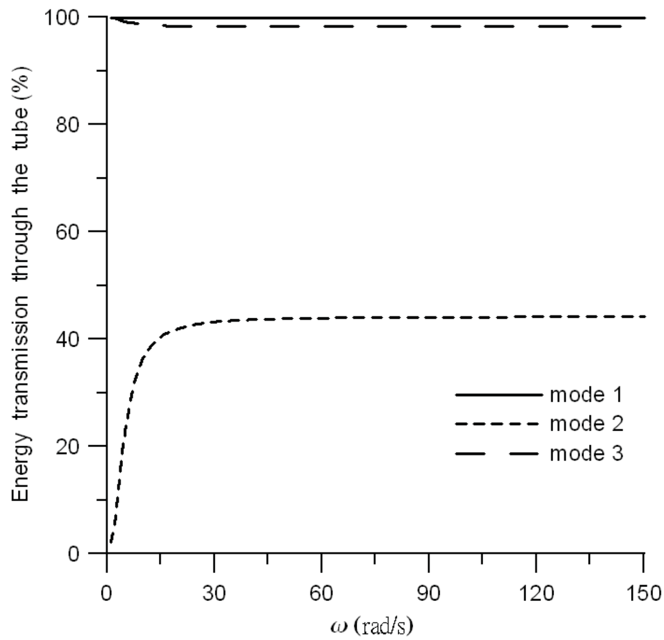

Figure 3: Relation between the energy propagation through the tube and the wave frequency.

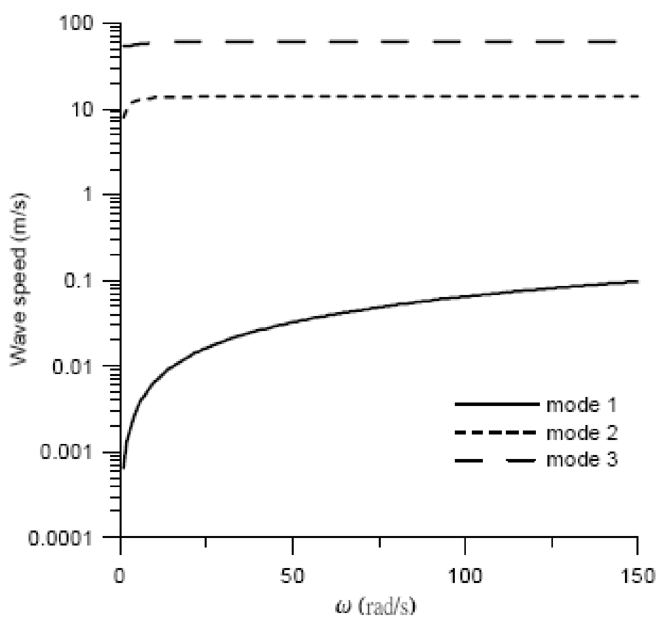

Figure 4: Relations between the frequency ω and three kinds of wave velocities c.

In other way, the wave speed of the Lamb mode in the Klip model (1968) is $c_0 = \sqrt{E/[\rho_f(1-\nu^2)]}$. Obviously, the corresponding wave speed is also independent to the wave frequency. This model is not applicable for determining the energy propagation. Considering the ratio h/R from 0.04 to 0.14, it is observed that the numerical results in the Klip model are slightly less than those determined by using the present method by 1.5%. Moreover, the wave speed is independent of the ratio 'h/R'. It is because the Lamb mode is the longitudinal wave propagation through the wall only and the flexural motion of a tube wall is not considered.

In addition to the Moens-Korteweg theory, several methods are used to investigate the dispersion curves of the Young mode shown in Figure 5. It is found that the wave speed determined by Wang et al. (1997) is overestimated and that by Cox (1970) is underestimated. Further, Figure 6 shows the relation between the transmission per wavelength and the wave frequency of the Young mode. It is observed that the transmission per wavelength increases with the wave frequency. If the wave frequency is large enough, the transmission per wavelength approaches constant. Moreover, it is found that the transmission determined by Wang et al. (1997) is over estimated.

Finally, the effects of the poison ratio of a tube ν, the viscosity of a liquid μ, and the pre-stressed pressure P_0 on the wave speeds and the energy dissipation of the three modes are investigated as follows: Unless the parameters are stated specially, all parameters are the same as those in Figure 2.

As to the first mode, it is found that the effects of the liquid viscosity μ, and the pre-stressed pressure P_0 on the wave speeds of the first mode are negligible. If the wave frequency is small, the wave speed of the first mode is independent of the Poisson ratio ν. But if the wave frequency is large, the wave speed will increase slightly with the Poisson ratio ν. Moreover, it is found that the energy transmission of the first mode is independent of these parameters.

As to the second mode, it is observed from Figure 7 that if the wave frequency is small, the effect of the liquid viscosity μ on the wave speed is obvious. On the other hand, when the wave frequency is large, the effect of the pre-stressed pressure P_0 is obvious. But the effect of the Poisson ratio ν on the wave speed is negligible. It is not presented here. Note that in the Moens-Korteweg theory the effects of the Poisson ratioν, the viscosity of a liquid μ, the pre-stressed pressure P_0, and the wave frequency on the wave speeds, are neglected. Therefore, by using the Moens-Korteweg theory one can derive only the relation between the ratio 'h/R' and the wave speed.

Moreover, it is found that the energy transmission of the second mode is independent of the pre-stressed pressure P_0. However, as shown in Figure 8, the energy

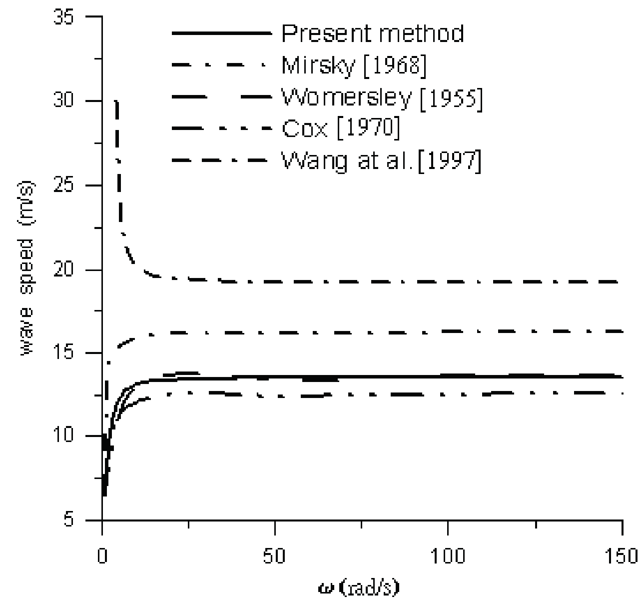

Figure 5: Comparison of wave speeds of the second mode in different models.

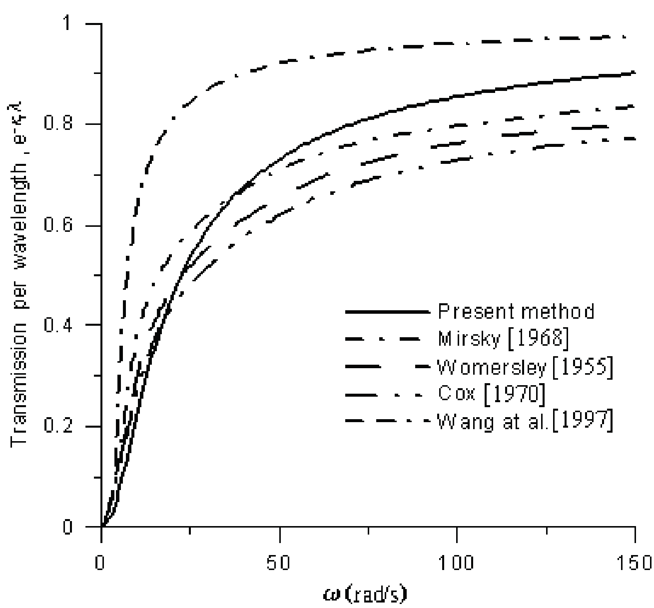

Figure 6: Comparison of dispersion curves of the second mode in different models.

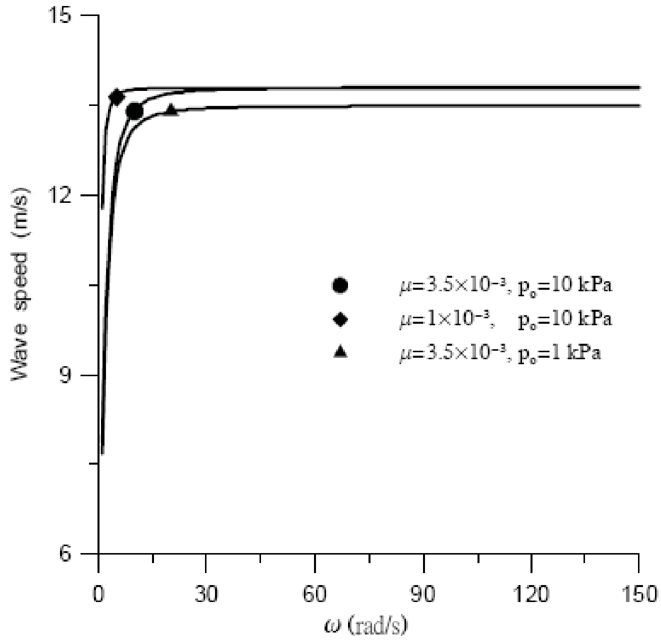

Figure 7: Influence of the pre-pressure p_0 and the kinetic viscosity μ of liquid on the wave speed of the second mode.

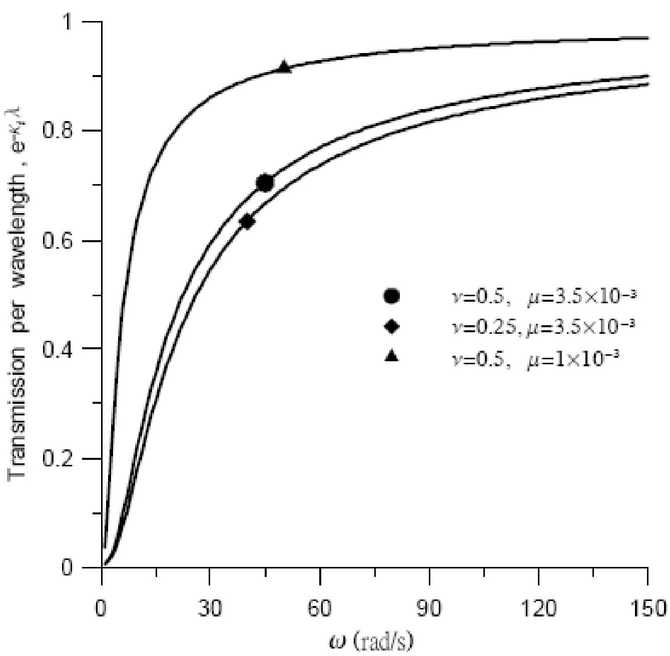

Figure 8: Influence of the Poisson ratio ν and the kinetic viscosity μ on the energy dispersion of the second mode.

transmission of the second mode increases greatly with the wave frequency. The effect of the Poisson ratio on the energy transmission is small. But the effect of the liquid viscosity μ is great. It is because more than a half of the wave energy of the second mode is transmitted through the liquid.

As to the third mode, Figure 9 shows that the effect of the Poisson ratio ν on the wave speed is great. The fact has been presented in the Klip model. When the wave frequency is small, the effect of the liquid viscosity μ on the wave speed is significant. However, the effect of the pre-stressed pressure P_0 is negligible. It is not presented here. Note that in the Klip theory the effects of the viscosity of a liquid μ, the pre-stressed pressure P_0, and the wave frequency on the wave speed are neglected. Therefore, by using the Klip theory one can derive only the relation between the Poisson ratio and the wave speed.

Finally, as shown in Figure 10, when the wave frequency is increased from zero, the energy transmission of the third mode is abruptly decreased. If the wave frequency is over a critical value, the energy transmission increases with the wave frequency. If the wave frequency is large enough, the energy transmission will be constant. This phenomenon of the third mode is greatly different to that of the first and second modes. Moreover, the effects of the Poisson ratio and the liquid viscosity on the energy transmission of the third mode are great.

6 Conclusion

In this paper, it presents a new theory simulating the wave propagation of a elastic tube conveying blood. The analytical solution of the system is derived. By using this new theory, the flexural, Young and Lamb modes can be obtained simultaneously. The effects of several important parameters on the wave propagation are investigated. It is found that

(1) Almost all the energies of the flexural and Lamb modes are transmitted through the tube. However, only about sixty percent of the energy of the Young mode is transmitted through the liquid.

(2) The energy transmission of the flexural mode is independent of the Poisson ratio ν, the liquid viscosity μ, and the pre-stressed pressure P_0, and the wave frequency ω.

(3) The energy transmission of the Young mode increases greatly with the wave frequency. The effect of the Poisson ratio on the energy transmission of the second mode is small.

(4) When the wave frequency is increased from zero, the energy transmission of

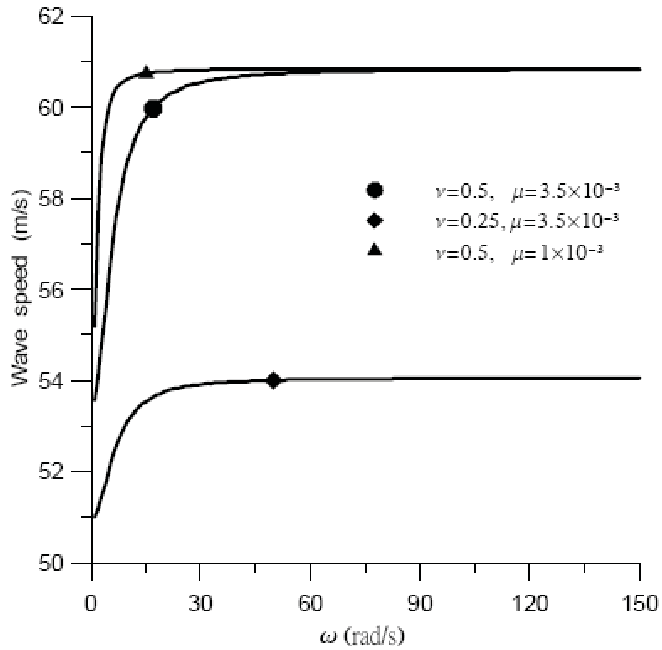

Figure 9: Influence of the kinetic viscosity μ and the Poisson ratio ν on the wave speed of the third mode.

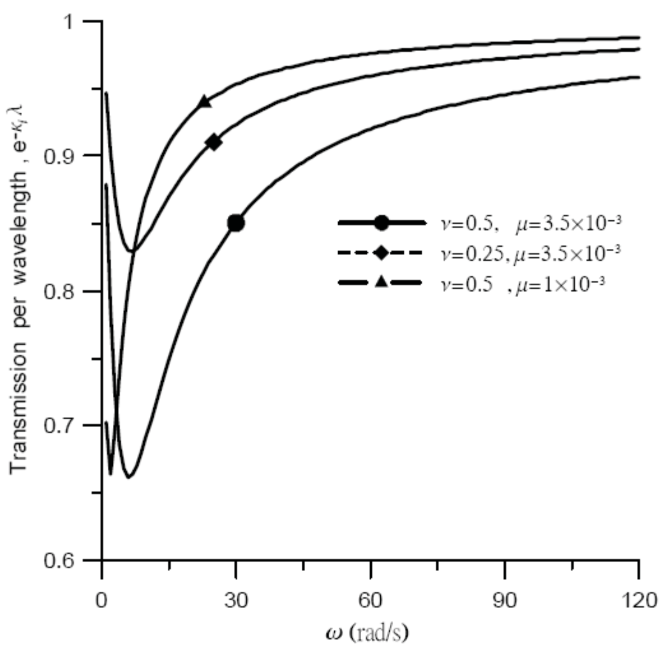

Figure 10: Influence of the Poisson ratio ν and the kinetic viscosity μ on the energy dispersion of the third mode.

the Lamb mode is abruptly decreased. If the wave frequency is over a critical value, increasing the wave frequency increases the energy transmission. Moreover, the effects of the Poisson ratio and the liquid viscosity on the energy transmission of the Lamb mode are great.

Acknowledgement: The support of the National Science Council of Taiwan, R. O. C., is gratefully acknowledged (Grant number: Nsc95-2212-E168-008).

References

Attinger, E. O. (1968): *Analysis of pulsatile blood flow. In Advances in Biomedical Engineering and Medical Physics*. (Edited by S. N. Levine), Interscience, New York.

Bergel, D. H. (1961): The dynamic elastic properties of the arterial wall. *Journal of Physiology*. 156: 458-469.

Cox, R. H. (1970): Wave propagation through a Newtonian fluid contained within a thick-walled viscoelastic tube: The influence of wall compressibility. *Biophys. J.* 3, 317-355.

Demiray, H. (1997): Wave in initially stressed fluid-filled thick tubes. *J. Biomechanics*, v30, n3, 273-276.

Dym, C. L. (1974): *Introduction to theory of shells*. Pergamon Press, Oxford.

Fishman, A. P.; Richards, D. W. (1964): *Circulation of the blood: Men and Ideas.* New York: Oxford University Press.

Hales, S. (1733): *Statical Essays: Containing Haemastaticks*.

Harvey, W. (1628): *Movement of the Heart and Blood in Animals*. William Fitzer, Frankurt.

Klip, W.; van Loon, P.; Klip, D. A. (1968): Formulas for phase velocity and damping of longitudinal waves in thick-walled viscous tubes," *J. Appl. Phys.* Vol. 38, 3745-3755.

Korteweg, D. J. (1878): Uber die Fortpflanzungsges-chwindigkeit des Schalles in elastischen Rohren. *Ann. Phys. Chem.* (NS) 5: 525.

Milnor, W. R. (1989): *Hemodynamics*, 2^{nd} Edition, William&Wilkins.

Mirsky, I. (1968): Wave propagation in a viscous fluid contained in an orthotropic elastic tube. *Biophys. J.* 7, 165-186.

Moens, A. I. (1878): *Die pulskurve*, Leiden.

Nichols, W. W.; O'Rourke, M. F. (1990): *McDonald's Blood Flow in Arteries: Theoretical, experimental and clinical principles*. 3^{rd} Edition, Philadelphia, London.

Sarkar, A.; Sonti, V. R. (2007): Asymptotic analysis for the coupled wavenumbers in an infinite fluid-filled flexible cylindrical shell: the axisymmetric mode. *CMES: Computer Modeling in Engineering & Science*, vol. 21, no. 3, pp.193-207.

Tsangaris, S.; Drikakis, D. (1989): Pulsating blood flow in an initially stressed, anisotropic elastic tube: Linear approximation of pressure waves. *Med. & Biol. Eng. & Comp.*, 27, 1, pp. 82-88.

Wang, Y. Y. L.; Chang, C. C.; Chen, J. C.; Hsiu, H.; Wang, W. K. (1997): Pressure wave propagation in a distensible tube arterial model with radial dilation. *IEEE Engineering in Med. Biol. Mag.*, pp. 51-56.

Wang, Y. Y. L.; Lia, W. C.; Hsiu, H.; Jan, M. Y.; Wang, W. K. (2000): Effect of length on the fundamental resonance frequency of arterial models having radial dilatation. *IEEE Trans. On Biomedical Eng.*, vol. 47, no. 3, pp. 313-318.

Womersley, J. R. (1955): Oscillatory motion of a viscous liquid in a thin-walled elastic tube.I. The linear approximation for long waves. *Phil. Mag.* vol. 46: pp. 199-221.

Yang, C.; Tang, D.; Yuan, C.; Hatsukami, T. S.; Zheng, J.; Woodard, P. K. (2007): In Vivo/Ex Vivo MRI-Based 3D non-Newtonian FSI models for human atherosclerotic plaques compared with fluid/wall-only models. *CMES: Computer Modeling in Engineering & Sciences*, vol.19, no.3, pp.233-245.